

Magneto-elastic coupling in multiferroic metal-organic framework $[(\text{CH}_3)_2\text{NH}_2]\text{Co}(\text{HCOO})_3$ EP

Cite as: AIP Advances 11, 015040 (2021); <https://doi.org/10.1063/9.0000147>

Submitted: 15 October 2020 . Accepted: 25 November 2020 . Published Online: 26 January 2021

 Komalavalli Thirunavukkumaras, Rachael Richardson, Zhengguang Lu, Dmitry Smirnov, Nan Huang, Nicholas Combs, Ganesh Pokharel, and David Mandrus

COLLECTIONS

Paper published as part of the special topic on [65th Annual Conference on Magnetism and Magnetic Materials](#)

 This paper was selected as an Editor's Pick



[View Online](#)



[Export Citation](#)



[CrossMark](#)

ARTICLES YOU MAY BE INTERESTED IN

[Thickness dependence of spin torque effect in Fe/MgO/Fe magnetic tunnel junction: Implementation of divide-and-conquer with first-principles calculation](#)
AIP Advances 11, 015036 (2021); <https://doi.org/10.1063/9.0000117>

[High-frequency magnetotransport in \$\text{La}_{1-x}\text{Sr}_x\text{MnO}_3\$ \(\$x = 0.12\text{-}0.20\$ \)](#)
AIP Advances 11, 015345 (2021); <https://doi.org/10.1063/9.0000107>

[Multiferroic and thermal expansion properties of metal-organic frameworks](#)
Journal of Applied Physics 127, 080901 (2020); <https://doi.org/10.1063/1.5137819>

Call For Papers!

AIP Advances

SPECIAL TOPIC: Advances in Low Dimensional and 2D Materials

Magneto-elastic coupling in multiferroic metal-organic framework $[(\text{CH}_3)_2\text{NH}_2]\text{Co}(\text{HCOO})_3$

Cite as: AIP Advances 11, 015040 (2021); doi: 10.1063/9.0000147

Presented: 2 November 2020 • Submitted: 15 October 2020 •

Accepted: 25 November 2020 • Published Online: 26 January 2021



View Online



Export Citation



CrossMark

Komalavalli Thirunavukkumaras, ^{1,a)}  Rachael Richardson, ¹ Zhengguang Lu, ² Dmitry Smirnov, ³ Nan Huang, ⁴ Nicholas Combs, ⁴ Ganesh Pokharel, ⁵ and David Mandrus ⁴

AFFILIATIONS

¹ Department of Physics, Florida A & M University, Tallahassee, Florida 32307, USA

² Department of Physics, Florida State University, Tallahassee, Florida 32306, USA

³ National High Magnetic Field Laboratory, Tallahassee, Florida 32310, USA

⁴ Department of Materials Science and Engineering, University of Tennessee Knoxville, Tennessee 37996, USA

⁵ Department of Physics and Astronomy, University of Tennessee Knoxville, Tennessee 37996, USA

Note: This paper was presented at the 65th Annual Conference on Magnetism and Magnetic Materials.

a) Author to whom correspondence should be addressed: komalavalli.thirunav@famu.edu

ABSTRACT

Metal-organic frameworks based on metal-formates have emerged as a intriguing class of multiferroics with wide range of applications. In this work, we present magneto-Raman spectroscopic investigations on $[(\text{CH}_3)_2\text{NH}_2]\text{Co}(\text{HCOO})_3$ belonging to this family. The spectroscopic studies were performed at magnetic fields up to 31 T at the temperature of 2.3 K. It was observed that the formate bending mode at around 798 cm^{-1} shifts to higher energies with increasing magnetic field. The magneto-response of the phonon also exhibits anomalies at magnetic fields of 14.5 T and 23.5 T corresponding to magnetic phase transitions. Based on our results, we conclude that the formate bending mode does play a role in facilitating the saturation of magnetic states similar to its Mn and Ni analogs.

© 2021 Author(s). All article content, except where otherwise noted, is licensed under a Creative Commons Attribution (CC BY) license (<http://creativecommons.org/licenses/by/4.0/>). <https://doi.org/10.1063/9.0000147>

I. INTRODUCTION

Metal-organic framework (MOF) is an interesting class of hybrid materials that have excellent applications in catalysis, gas storage and sensors, drug delivery and many more.^{1–4} With the explosion of the field of multiferroics,⁵ MOFs became one of the sought after approaches to obtain materials that have at least two coexisting magnetic, electric and/or elastic orders.^{6–8} This quest for multiferroics in MOFs achieved its first success with the discovery of multiferroicity in the family of perovskite MOFs.⁹ Since then, several intriguing magnetic and ferroelectric properties were reported in this subgroup of metal formate MOFs.^{7,10–22}

The family of metal formates has the general formula $[(\text{CH}_3)_2\text{NH}_2]\text{M}(\text{HCOO})_3$ where $\text{M}=\text{Fe}^{2+}$, Mn^{2+} , Co^{2+} , Ni^{2+} , Zn^{2+} ,

Mg^{2+} , Cu^{2+} , Cd^{2+} . Initially, these MOFs were classified as Type-I multiferroics where the electric and magnetic order have different mechanisms. The ferroelectric order was associated with the order-disorder transitions of the $[(\text{CH}_3)_2\text{NH}_2]^+$ cations while the magnetic order was attributed to the $[\text{M}(\text{HCOO})_3]^-$ ions.^{9,10,17} However, more recently a coupling between the magnetic and ferroelectric order was observed in Mn-,¹⁶ Fe-¹⁸ and also Co-²³ based compounds. These results indicate that they rather exhibit Type-II multiferroics behavior. Mn-, Co- and Ni-based compounds are canted weak ferromagnets with T_c values of 8.5 K, 14.9 K and 35.6 K, respectively.²⁴

The $[(\text{CH}_3)_2\text{NH}_2]\text{Co}(\text{HCOO})_3$ (Co-MOF) is particularly intriguing due to the observation of two co-existing phases with the canted magnetically-ordered phase²⁵ and glassy behavior.¹⁹ Recent investigations on structure-property relationship suggest that the

Co-MOF adopts a different mechanism to facilitate the transition to their fully saturated magnetic states unlike Mn- and Ni-based compounds which rely on formate bending mode for magneto-elastic coupling.²² In this article, we report the Raman spectroscopic investigations on $[(\text{CH}_3)_2\text{NH}_2]\text{M}(\text{HCOO})_3$ with $\text{M}=\text{Co}^{2+}$ (Co-MOF) at high magnetic fields that were performed to further probe the nature of magneto-elastic coupling in this intriguing family of MOFs.

II. EXPERIMENT

Co-MOF samples were synthesized using a solvothermal method.⁹ The yield consisted of pink-orange crystals of about $500 \mu\text{m}^{-1}$ mm dimension. The samples were found to be sensitive to ambient conditions (oxygen and/or moisture). Careful sample handling procedures were therefore followed during the preparation for every spectroscopic measurement.

Raman spectroscopic experiments at magnetic fields were performed using two different magnet systems in National High Magnetic Field Laboratory. The data was acquired in 31 T resistive magnet as well as 17.5 T superconducting magnet. This allowed detailed experiments below and above 17.5 T as well as check reproducibility of data. The experiment was performed using 532 nm laser excitation source with incident power of about 50 μW . The laser beam was coupled to a custom-built fiber-based probe for 31 T magnet. The excitation light fed into the magnet via a single mode excitation fiber was focused on to the sample by an aspheric objective lens ($\text{NA} = 0.67$) to a spot size of $3.5 \mu\text{m}$ in diameter. The scattered light was collected using the same lens and coupled to the spectrometer with a liquid nitrogen cooled CCD through a collection fiber with $100 \mu\text{m}$ diameter. Spectrometer with 1800g/mm grating and 0.75 m focal distance from Princeton instrument was used for the measurement to achieve a spectral resolution of about 1 cm^{-1} . The spectra were recorded for magnetic fields up to 31 T at lowest stable temperature of 2.3 K.

III. RESULTS AND DISCUSSION

Co-MOF crystallizes in trigonal symmetry in space group $\text{R}\bar{3}c$ with $Z=6$.^{9,19,32} The crystal structure visualized along the three crystallographic directions are shown in Fig. 1(a)-(c). The crystal

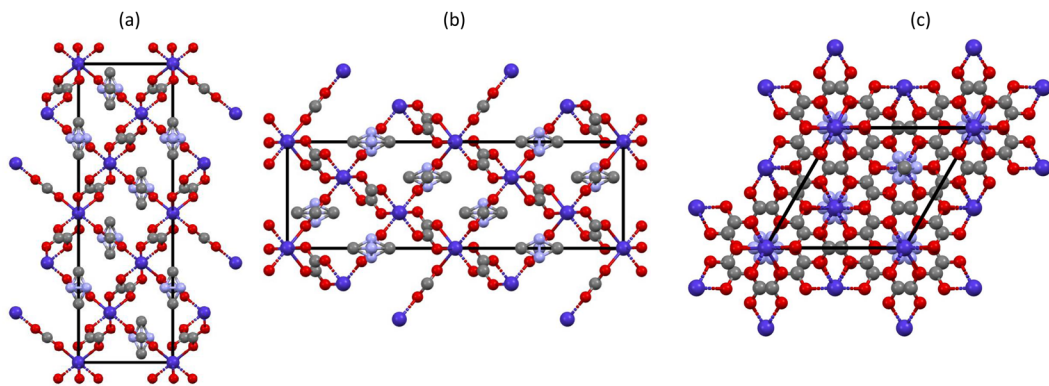


FIG. 1. The crystal structures of $[(\text{CH}_3)_2\text{NH}_2]\text{Co}(\text{HCOO})_3$ viewed along the crystallographic axes a, b and c, revealing the view of (a) bc plane, (b) ac plane and (c) ab plane, respectively are shown.

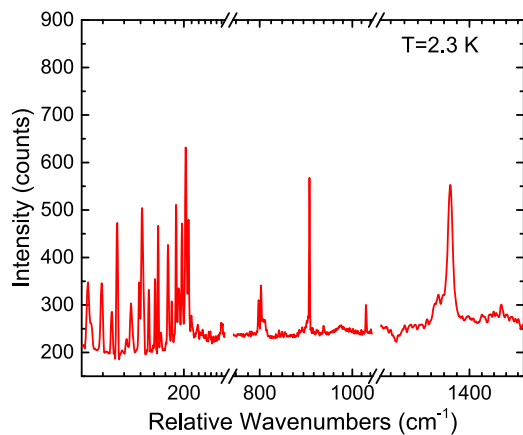


FIG. 2. The Raman spectrum of Co-MOF acquired at $T=2.3 \text{ K}$ at zero magnetic field.

consists of cobalt (Co^{2+} cation, formate (HCOO^-) anion and the organic DMA ($(\text{CH}_3)_2\text{NH}_2^+$ cation. The cobalt ions are connected to the nearest neighbor metal ion via formate bridges and is positioned in CoO_6 environment. The DMA cation occupies the cavity of the metal-formate framework.

The Raman spectrum of Co-MOF below 1500 cm^{-1} at lowest measured temperature of 2.3 K in the absence of magnetic field is shown in Fig. 2. While some of the very weak phonon modes are not visible in the spectrum due to reduced collection efficiency of Raman setup inside a high-field magnet, most of the expected phonon modes were observed. The observed phonon modes, their assignment along with the nature of vibrations are listed in Table I. The vibrational modes of Co-MOF can be divided into internal vibrations of DMA⁺ and formate ions, and the lattice vibrations involving these ions and Co²⁺ cations.²⁶⁻²⁸ Free HCOO⁻ ion has six internal modes while free DMA⁺ ion (C_{2v} symmetry) has 27 internal modes.^{29,30} Previous calculations of vibrational properties of Ni-MOF also show that there are 69 expected vibrational modes of $[\text{M}(\text{CHOO})_6]^{4-}$ complex.²⁶ The internal modes of the ions and the lattice vibrations are observed at frequencies above and below

TABLE I. The table shows the Raman active phonons below 1400 cm⁻¹ observed at 2.3K and their assignment. The assignments were determined by comparison with the phonons assignments published for other transition metal analogs with Mg, Cd, Zn, Fe and Ni.²⁶⁻³¹

Observed ^a	Assignment	Vibration
1458vw	$\delta_{as}(\text{CH}_3)$	Antisymmetric bending CH ₃
1366	$\nu_5(\text{HCOO}^-)$	In-plane bending C-H
1345	$\nu_2(\text{HCOO}^-)$	Symmetric stretching C-O
1034	$\nu_{as}(\text{CNC})$	Antisymmetric stretching
933	$\rho(\text{NH}_2)$	Rocking NH ₂
902	$\nu_5(\text{CNC})$	Symmetric stretching
810sh 806sh	$\nu_3(\text{HCOO}^-)$	Symmetric bending O-C-O
798 802	$\nu_3(\text{HCOO}^-)$	Symmetric bending O-C-O
411w	$\delta(\text{CNC})\text{T}(\text{Co}^{2+})$	Bending
332vw	$\tau(\text{CH}_3)\text{T}(\text{Co}^{2+})$	Torsion
258vw	T (Co ²⁺)	Translation
242vw	T (Co ²⁺)	Translation
221w	T (HCOO ⁻)	Translation
213	T (HCOO ⁻)	Translation
205	T (HCOO ⁻)	Translation
195	L (HCOO ⁻)	Libration
186 188	L (HCOO ⁻)	Libration
180	L (HCOO ⁻)	Libration
170	L (DMA)	Libration
161	L (DMA)	Libration
147w	L (DMA)	Libration
141	L (DMA)	Libration
135	L (DMA)	Libration
125	L (HCOO ⁻)	Libration
113	L (HCOO ⁻)	Libration
109	L (HCOO ⁻)	Libration
98 92w 81	T (DMA)	Translation
75	$\delta(\text{CoOC})$	Bending of Co-O-C
66	$\delta(\text{CoOC})$	Bending of Co-O-C
57sh 55	$\delta(\text{CoOC})$	Bending of Co-O-C

^ash-shoulder, vw-very weak and w-weak.

800 cm⁻¹, respectively. The vibrational modes above 800 cm⁻¹ mainly correspond to the symmetric and antisymmetric stretching and bending of formate ion. Although the modes observed in the infrared and Raman spectra are generally governed by mutual exclusion due to selection rules, most of the internal vibrational modes of the ions were observed in both infrared and Raman spectra. The observation of the internal modes of formate ions and DMA⁺ ion at very similar wavenumbers in infrared and Raman spectra were attributed due to weak intermolecular interactions and disorder-induced relaxation of selection rules, respectively.³¹

With the application of magnetic fields, the vibrational modes of Co-MOF remained unchanged except for one vibrational mode at around 798 cm⁻¹ corresponding to the symmetric bending of -O-C-O- in the formate ion. The magnetic field dependence of this symmetric bending mode is shown in Fig. 3. The mode exhibited a small shift to increasing energies with increasing magnetic fields up to 31 T. The changes with respect to the applied magnetic fields lower than 25 T were rather small in comparison to those at higher magnetic fields. The magnetic field induced changes of the bending

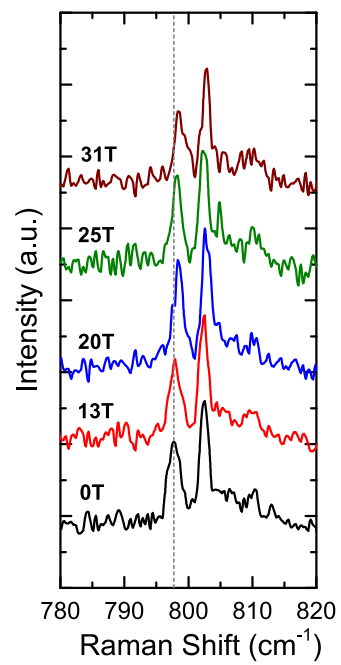


FIG. 3. The magnetic field dependent changes in the phonons around 800 cm⁻¹ in the magnetic field range from 0 T to 31 T are plotted with vertical offset. Only selected magnetic field values are shown for clarity.

mode can be better understood in Fig. 4. The total change in the energy of the vibrational mode is about 134 μ eV corresponding to a temperature change of 1.56 K. Although the change is very small, it is consistent with magnetic field induced response in infrared spectroscopic investigation²² and observed to be extremely reproducible with magnetic field increase. Furthermore, the phonon shifts were not observed at even slightly higher temperature of 5 K indicating that highly stable lower temperatures and magnetic fields are required to observe these small changes. The width of the vibrational

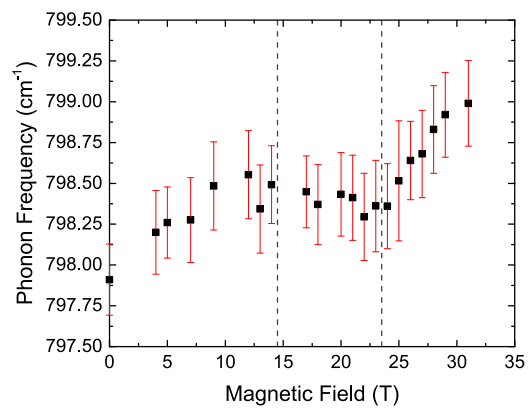


FIG. 4. The change in energy of the formate bending mode is shown as a function of magnetic field. The vertical dashed lines indicate the magnetic fields at which magnetic phase transitions have been observed in magnetization and electric polarization measurements.²³

mode did not exhibit any discernable change in response to external magnetic field.

The slope of the field induced changes were observed to change at two magnetic fields around 14.5 T and 23.5 T. The shift of the phonon modes is nearly linear at magnetic field above 23.5 T. Recent magnetization measurements have revealed that Co-MOF undergoes a transition from weak ferromagnetic phase to spin-flop phase at around 14.5 T when magnetic field was applied along the [010] crystallographic direction.²³ A phase diagram of Co-MOF constructed based on data from magnetization and electric polarization measurement also indicate a transition from spin-flop phase to paramagnetic phase close to 23.5 T for magnetic field along [010].²³ Although we do not know the precise direction of applied magnetic field with respect to crystallographic orientation in our experiments, the anomalies in the phonon energy is in excellent agreement with the previous report. This observation also indicates that the applied magnetic field is along the easy axis [010].

In the magneto-infrared studies on Mn-, Ni- and Co-MOFs, it was observed that -O-C-O- formate bending mode is the only phonon that is sensitive to applied field in case of Mn-MOF.²² This observation was indicated as evidence for magnetic-elastic coupling facilitating Mn-O-C-O-Mn superexchange pathway.²¹ Based on the temperature and magnetic field dependence of the infrared spectra of these MOFs, it was suggested that Mn-MOF and Ni-MOF are quite similar in terms of magneto-elastic coupling. In the same study, the formate bending mode of Co-MOF did not show any magneto-response. It was concluded that the magneto-elastic coupling in Co-MOF is different from that of Mn- and Ni-MOF due to distortions in the CoO_6 octahedra that were causing the inherent differences in these compounds. However, the observation of magnetic-field induced shifts in the formate bending mode in the Raman experiments presented here indicates that the nature of the magneto-elastic coupling is not different from those of the other analogs even though the energy scale is altered due to the octahedral distortions.

IV. CONCLUSION

Magneto-Raman spectroscopic studies of Co-MOF at magnetic fields up to 31 T were performed at temperature of 2.3 K. We find that the formate bending mode at frequency of about 798 cm^{-1} is the only phonon sensitive to the external magnetic field. The energy of formate bending mode shifts to higher frequencies with increasing magnetic field. In addition, the magneto-response of this phonons exhibits anomalies at 14.5 T and 23.5 T corresponding to magnetic phase transitions from weak ferromagnetic phase to spin-flop phase and from spin-flop phase to paramagnetic state, respectively. This shift in phonon energy also signifies that formate bending mode definitely plays a mode in facilitating saturation of magnetic states in this compound. The difference in the energy scale of the coupling in comparison with the Mn-MOF and Ni-MOF is most probably due to the octahedral distortions observed in Co-MOF.

ACKNOWLEDGMENTS

KT acknowledges funding from Department of Navy's historically black colleges and universities and minority institutions (HBCU/MI) program award number N00014-17-1-3061. This work was performed at the National High Magnetic Field Laboratory

which is supported by the National Science Foundation through NSF/DMR-1644779 and the state of Florida.

DATA AVAILABILITY

The data that support the findings of this study are available from the corresponding author upon reasonable request.

REFERENCES

- 1 C. Sanchez, B. Julián, P. Belleville, and M. Popall, "Applications of hybrid organic-inorganic nanocomposites," *Journal of Materials Chemistry* **15**, 3559–3592 (2005).
- 2 L. E. Kreno, K. Leong, O. K. Farha, M. Allendorf, R. P. Van Duyne, and J. T. Hupp, "Metal-organic framework materials as chemical sensors," *Chemical Reviews* **112**, 1105–1125 (2012).
- 3 H. Furukawa, K. E. Cordova, M. O'Keeffe, and O. M. Yaghi, "The chemistry and applications of metal-organic frameworks," *Science* **341**, 1230444 (2013).
- 4 Y. Zhao, "Emerging applications of metal-organic frameworks and covalent organic frameworks," *Chemistry of Materials* **28**, 8079–8081 (2016).
- 5 S.-W. Cheong and M. Mostovoy, "Multiferroics: A magnetic twist for ferroelectricity," *Nature Materials* **6**, 13–20 (2007).
- 6 R. Ramesh, "Materials science: Emerging routes to multiferroics," *Nature* **461**, 1218 (2009).
- 7 G. Rogez, N. Viart, and M. Drillon, "Multiferroic materials: The attractive approach of metal-organic frameworks (MOFs)," *Angewandte Chemie International Edition* **49**, 1921–1923 (2010).
- 8 E. Pardo, C. Train, H. Liu, L.-M. Chamoreau, B. Dkhil, K. Boubekeur, F. Lloret, K. Nakatani, H. Tokoro, S.-I. Ohkoshi, and M. Verdaguer, "Multiferroics by rational design: Implementing ferroelectricity in molecule-based magnets," *Angewandte Chemie International Edition* **51**, 8356–8360 (2012).
- 9 P. Jain, V. Ramachandran, R. J. Clark, H. D. Zhou, B. H. Toby, N. S. Dalal, H. W. Kroto, and A. K. Cheetham, "Multiferroic behavior associated with an order-disorder hydrogen bonding transition in metal-organic frameworks (MOFs) with the perovskite ABX_3 architecture," *Journal of the American Chemical Society* **131**, 13625–13627 (2009).
- 10 G.-C. Xu, W. Zhang, X.-M. Ma, Y.-H. Chen, L. Zhang, H.-L. Cai, Z.-M. Wang, R.-G. Xiong, and S. Gao, "Coexistence of magnetic and electric orderings in the metal-formate frameworks of $[\text{NH}_4][\text{M}(\text{HCOO})_3]$," *Journal of American Chemical Society* **133**, 14948–14951 (2011).
- 11 L. Canñadillas-Delgado, O. Fabelo, J. Alberto Rodríguez-Velamazán, M. Lemée-Cailleau, S. A. Mason, E. Pardo, F. Lloret, J.-P. Zhao, X.-H. Bu, V. Simonet, C. V. Colin, and J. Rodríguez-Carvajal, "The role of order-disorder transitions in the quest for molecular multiferroics: Structural and magnetic neutron studies of a mixed valence iron(II)-Iron(III) formate framework," *Journal of American Chemical Society* **134**, 19772–19781 (2012).
- 12 A. Stroppa, P. Jain, P. Barone, M. Marsman, J. M. Perez-Mato, A. K. Cheetham, H. W. Kroto, and S. Picozzi, "Electric control of magnetization and interplay between orbital ordering and ferroelectricity in a multiferroic metal-organic framework," *Angewandte Chemie International Edition* **50**, 5847–5850 (2011).
- 13 D.-W. Fu, W. Zhang, H.-L. Cai, Y. Zhang, J.-Z. Ge, R.-G. Xiong, S. D. Huang, and T. Nakamura, "A multiferroic perdeutero metal-organic framework," *Angewandte Chemie, International Edition* **50**, 11947–11951 (2011).
- 14 A. Stroppa, P. Barone, P. Jain, J. M. Perez-Mato, and S. Picozzi, "Hybrid improper ferroelectricity in a multiferroic and magnetoelectric metal-organic framework," *Advanced Materials* **25**, 2284–2290 (2013).
- 15 D. Di Sante, A. Stroppa, P. Jain, and S. Picozzi, "Tuning the ferroelectric polarization in a multiferroic metal-organic framework," *J. Am. Chem. Soc.* **135**, 18126 (2013).
- 16 W. Wang, L.-Q. Yan, J.-Z. Cong, Y.-L. Zhao, F. Wang, S.-P. Shen, T. Zou, D. Zhang, S. G. Wang, X. F. Han, and Y. Sun, "Magnetoelectric coupling in the paramagnetic state of a metal-organic framework," *Scientific Reports* **3**, 2024 (2013).

¹⁷B. Pato-Doldán, L. C. Gómez-Aguirre, J. M. Bermúdez-García, M. Sánchez-Andújar, A. Fondado, J. Mira, S. Castro-García, and M. A. Señaris-Rodríguez, “Coexistence of magnetic and electrical order in the new perovskite-like $(C_3N_2H_5)[Mn(HCOO)_3]$ formate,” *RSC Advances* **3**, 22404–22411 (2013).

¹⁸Y. Tian, A. Stroppa, Y. Chai, L. Yan, S. Wang, P. Barone, S. Picozzi, and Y. Sun, “Cross coupling between electric and magnetic orders in a multiferroic metal-organic framework,” *Scientific Reports* **4**, 6062 (2014).

¹⁹R. Yadav, D. Swain, H. L. Bhat, and S. Elizabeth, “Order-disorder phase transition and multiferroic behaviour in a metal organic framework compound $(CH_3)_2NH_2Co(HCOO)_3$,” *Journal of Applied Physics* **119**, 064103 (2016).

²⁰A. J. Clune, K. D. Hughey, C. Lee, N. Abhyankar, X. Ding, N. S. Dalal, M. Whangbo, J. Singleton, and J. Musfeldt, “Magnetic field-temperature phase diagram of multiferroic $[(CH_2)_3NH_2]Mn(HCOO)_3$,” *Physical Review B* **96**, 104424 (2017).

²¹K. D. Hughey, A. J. Clune, M. O. Yokosuk, A. Al-Wahish, K. R. O’Neal, S. Fan, N. Abhyankar, H. Xiang, Z. Li, J. Singleton, N. S. Dalal, and J. L. Musfeldt, “Phonon mode links ferroicities in multiferroic $[(CH_3)_2NH_2]Mn(HCOO)_3$,” *Physical Review B* **96**, 180305 (2017).

²²K. D. Hughey, A. J. Clune, M. O. Yokosuk, J. Li, N. Abhyankar, X. Ding, N. S. Dalal, H. Xiang, D. Smirnov, J. Singleton, and J. L. Musfeldt, “Structure-property relations in multiferroic $[(CH_2)_3NH_2]M(HCOO)_3$ ($M = Mn, Co, Ni$),” *Inorganic Chemistry* **57**, 11569–11577 (2018).

²³L. C. Gómez-Aguirre, B. Pato-Doldán, J. Mira, S. Castro-García, M. A. Señaris-Rodríguez, M. Sánchez-Andújar, J. Singleton, and V. S. Zapf, “Magnetic ordering-induced multiferroic behavior in $[(CH_2)_3NH_2]Co(HCOO)_3$ metal-organic framework,” *J. Am. Chem. Soc* **138**, 1122–1125 (2016).

²⁴X.-Y. Wang, L. Gan, S.-W. Zhang, and S. Gao, “Perovskite-like metal formates with weak ferromagnetism and as precursors to amorphous materials,” *Inorganic Chemistry* **43**, 4615–4625 (2004).

²⁵K. Vinod, C. S. Deepak, S. Sharma, D. Sornadurai, A. T. Satya, T. R. Ravindran, C. S. Sundar, and A. Bharathi, “Magnetic behavior of the metal-organic framework $[(CH_3)_2NH_2]Co(HCOO)_3$,” *RSC Advances* **5**, 37818–37822 (2015).

²⁶M. Maczka, W. Zierkiewicz, D. Michalska, and J. Hanuza, “Vibrational properties and DFT calculations of the perovskite metal formate framework of $[(CH_2)_3NH_2][Ni(HCOO)_3]$ system,” *Spectrochimica Acta Part A: Molecular and Biomolecular Spectroscopy* **128**, 674–680 (2014).

²⁷M. Maczka, M. Ptak, and L. Macalik, “Infrared and Raman studies of phase transitions in metal-organic frameworks of $[(CH_3)_2NH_2][M(HCOO)_3]$ with $M=Zn, Fe$,” *Vibrational Spectroscopy* **71**, 98–104 (2014).

²⁸M. Maczka, T. A. Da Silva, W. Paraguassu, M. Ptak, and K. Hermanowicz, “Raman and IR studies of pressure- and temperature-induced phase transitions in $[(CH_2)_3NH_2][Zn(HCOO)_3]$,” *Inorganic Chemistry* **53**, 12650–12657 (2014).

²⁹M. Maczka, T. Almeida Da Silva, W. Paraguassu, and K. Pereira Da Silva, “Raman scattering studies of pressure-induced phase transitions in perovskite formates $[(CH_2)_3NH_2][Mg(HCOO)_3]$ and $[(CH_2)_3NH_2][Cd(HCOO)_3]$,” *Spectrochimica Acta Part A: Molecular and Biomolecular Spectroscopy* **156**, 112–117 (2015).

³⁰A. Ciupa, M. Maczka, A. Gągor, A. Pikul, E. Kucharska, J. Hanuza, and A. Sieradzki, “Synthesis, crystal structure, magnetic and vibrational properties of formamidine-templated Co and Fe formates,” *Polyhedron* **85**, 137–143 (2015).

³¹K. Szymborska-Malek, M. Trzebiatowska-Gusowska, M. Maczka, and A. Gągor, “Temperature-dependent IR and Raman studies of metal-organic frameworks $[(CH_3)_3NH_2][M(HCOO)_3]$, $M = Mg$ and Cd ,” *Spectrochimica Acta Part A: Molecular and Biomolecular Spectroscopy* **159**, 35–41 (2016).

³²P. Jain, N. S. Dalal, B. H. Toby, H. W. Kroto, and A. K. Cheetham, “Order-disorder antiferroelectric phase transition in a hybrid inorganic-organic framework with the perovskite architecture,” *Journal of American Chemical Society* **130**, 10450–10451 (2008).